biostabilisation and the role of carbohydrates. In: Amorphous food and pharmaceutical systems. Cambridge UK: The Royal Society of Chemistry, pp 73–87.
3. Yoshioka S, Aso Y. 2005. A quantitative assessment of the significance of molecular mobility as a determinant for the stability of lyophilized insulin formulations. Pharm Res 22:1358–1364.
4. Yoshioka S, Aso Y, Miyazaki T. 2006. Negligible contribution of molecular mobility to the degradation rate of insulin lyophilized with poly(vinylpyrrolidone). J Pharm Sci 95:939–943.
5. Yoshioka S, Miyazaki T, Aso Y. 2006. β-relaxation of insulin molecule in lyophilized formulations containing trehalose or dextran as a determinant of chemical reactivity. Pharm Res 23:961–966.
6. Collins F C, Kimball GE. 1949. Diffusion-controlled reaction rates. J Colloid Sci 4:425–437.
7. Craig ID, Parker R, Rigby NM, Cairns P, Ring SG. 2001. Maillard reaction kinetics in model preservation systems in the vicinity of the glass transiton: Experiment and theory. J Agric Food Chem 49: 4706–4712.
8. Guo Y, Byrn SR, Zografi G. 2000. Physical characteristics and chemical degradation of amorphous quinapril hydrochloride. J Pharm Sci 89: 128–143.
9. Giammona G, Carlisi B, Palazzo S. 1987. Reaction of a,b-poly(N-2-hydroxy)-DL-aspartamide with derivatives of carboxylic acid. J Polym Sci Polym Chem Ed 25:2813–2818.
10. Fujara F, Geil B, Sillescu H, Fleischer G. 1992. Translational and rotational diffusion in supercooled orthoterphenyl close to the glass transition. Z Phys B-Condensed Matter 88:195–204.

Pharmaceutical Research, Vol. 23, No. 5 May 2006 (© 2006)
DOI: 10.1007/s11095-006-9907-3

Research Paper

β-Relaxation of Insulin Molecule in Lyophilized Formulations Containing Trehalose or Dextran as a Determinant of Chemical Reactivity

Sumie Yoshioka,[1,2] Tamaki Miyazaki,[1] and Yukio Aso[1]

Received October 13, 2005; accepted January 6, 2006

Purpose. The purpose of this study was to elucidate whether the degradation rate of insulin in lyophilized formulations is determined by matrix mobility, as reflected in glass transition temperature (T_g), or by β-relaxation, as reflected in rotating-frame spin-lattice relaxation time ($T_{1\rho}$).
Methods. The storage stability of insulin lyophilized with dextran was investigated at various relative humidities (RH; 12–60%) and temperatures (40–90°C) and was compared with previously reported data for insulin lyophilized with trehalose. Insulin degradation was monitored by reverse-phase high-performance liquid chromatography. Furthermore, the $T_{1\rho}$ of the insulin carbonyl carbon in the lyophilized insulin–dextran and insulin–trehalose systems was measured at 25°C by ^{13}C solid-state NMR, and the effect of trehalose and dextran on $T_{1\rho}$ was compared at various humidities.
Results. The degradation rate of insulin lyophilized with dextran was not significantly affected by the T_g of the matrix, even at low humidity (12% RH), in contrast to that of insulin lyophilized with trehalose. The insulin–dextran system exhibited a substantially greater degradation rate than the insulin–trehalose system at a given temperature below the T_g. The difference in degradation rate between the insulin–dextran and insulin–trehalose systems observed at 12% RH was eliminated at 43% RH. In addition, the $T_{1\rho}$ of the insulin carbonyl carbon at low humidity (12% RH) was prolonged by the addition of trehalose, but not by the addition of dextran. This difference was eliminated at 23% RH, at which point the solid remained in the glassy state. These findings suggest that the β-relaxation of insulin is inhibited by trehalose at low humidity, presumably as a result of insulin–trehalose interaction, and thus becomes a rate determinant. In contrast, dextran, whose ability to interact with insulin is thought to be less than that of trehalose, did not inhibit the β-relaxation of insulin, and thus, the chemical activational barrier (activation energy) rather than β-relaxation becomes the major rate determinant.
Conclusions. β-Relaxation rather than matrix mobility seems to be more important in determining the stability of insulin in the glassy state in lyophilized formulations containing trehalose and dextran.

KEY WORDS: β-relaxation; glass transition; insulin; lyophilized formulation; molecular mobility; solid-state stability.

INTRODUCTION

An increasing number of studies have demonstrated that the chemical stability of drugs in amorphous solids is closely related to matrix mobility. Good correlations between chemical reaction rate and structural relaxation time have been reported for low molecular weight drugs, such as cephalosporins (1), quinapril (2), and aspirin (3), as well as for peptides and proteins, such as a monoclonal antibody (4), IgG1 antibody, and human growth hormone (1,5), and it has been found that the reaction rate constant increases proportionally with structural relaxation time.

On the other hand, other reports show no correlation between chemical stability and matrix mobility. The inactivation of enzymes lyophilized with various excipients is not related to matrix T_g (6–8). The scale of motion required for a given chemical reaction is considered to be one of the most important factors that determine whether chemical stability is correlated with matrix mobility. Chemical reactions that require translational or rotational motion of the entire molecule may exhibit close correlations with matrix mobility, whereas those that require small-scale motion of specific portions of the molecule may not. Recently, β-relaxation, the scale of which is smaller than matrix mobility (α-relaxation), has attracted attention as a molecular motion that determines the stability of amorphous glassy solids more directly than matrix mobility (9). However, little data are available that show direct correlations between chemical stability and β-relaxation.

The purpose of this study is to examine the relationship between chemical stability and β-relaxation in lyophilized insulin formulations, as compared with the relationship between chemical stability and matrix mobility. A previous study with insulin lyophilized from an acidic trehalose

[1] National Institute of Health Sciences, 1-18-1 Kamiyoga, Setagaya-ku, Tokyo 158-8501, Japan.
[2] To whom correspondence should be addressed. (e-mail: yoshioka@nihs.go.jp)

solution showed that the rates of A21-desamido insulin formation and dimerization via a cyclic intermediate depended on matrix mobility as indicated by T_g under low humidity conditions, but not under high humidity conditions (10). In this study, rotating-frame spin-lattice relaxation time ($T_{1\rho}$), which effectively detects molecular motions on the timescale of 10^{-5} s and reflects β-relaxation (11), was measured by ^{13}C solid-state NMR for insulin lyophilized with trehalose. Furthermore, the storage stability and β-relaxation of insulin lyophilized with dextran, whose ability to interact with proteins is thought to be less than that of trehalose, were investigated under various temperature and humidity conditions and were compared with those of insulin lyophilized with trehalose, to elucidate the relationship between chemical stability and β-relaxation.

MATERIALS AND METHODS

Preparation of Lyophilized Insulin Formulations

Lyophilized insulin formulations containing dextran were prepared as reported (10). Human zinc insulin (Humulin® RU-100) was purchased from Eli Lilly & Co. (Indianapolis, IN, USA) and converted into the zinc-free neutral form by dialysis as reported (12). Dextran 40k (D-4133, Sigma Chemical Co., St. Louis, MO, USA) was dissolved in the zinc-free insulin solution to make a 5 mg/mL solution, and the pH was adjusted to pH 4.0. The resulting solution contained insulin and dextran (1:1.5 w/w). Four hundred microliters of the solution was frozen in a polypropylene sample tube (10 mm in diameter) and then dried at a vacuum level below 5 Pa. Comparison of the amount of insulin before and after freeze drying indicated no significant degradation during freeze drying. Lyophilized samples with various water contents were obtained by storage at 15°C for 24 h in a desiccator with a saturated solution of $LiCl{\cdot}H_2O$ [12% relative humidity (RH)], $K_2CO_3{\cdot}2H_2O$ (43% RH), or $NaBr{\cdot}2H_2O$ (60% RH).

Lyophilized insulin formulations containing trehalose for $T_{1\rho}$, water absorption, and T_g measurements were prepared similarly as the insulin–dextran system, using trehalose (203-02252, Wako Pure Chemical Ind. Ltd, Osaka, Japan) instead of dextran. Similarly, lyophilized insulin alone was prepared without excipients, and lyophilized trehalose alone or dextran alone samples for water absorption and T_g measurements were prepared similarly without insulin.

Similar freeze drying was performed to prepare lyophilized poly-L-glutamic acid (PGA)–dextran or PGA–trehalose samples for $T_{1\rho}$ measurements, using PGA sodium (P-4764, Sigma Chemical Co.) instead of insulin.

Determination of T_g by Differential Scanning Calorimetry

The T_g of the lyophilized insulin formulations containing dextran was determined by modulated temperature differential scanning calorimetry (2920; TA Instruments, Newcastle, DE, USA), as reported (13). The conditions were as follows: a modulation period of 100 s, a modulation amplitude of ±0.5°C, and an underlying heating rate of 1°C/min. Samples were put in a hermetic pan. Temperature calibration was performed using indium. The samples, preequilibrated at 12, 43, and 60% RH, exhibited a T_g value of 107, 48, and 33°C, respectively. The observed single glass transition suggests that phase separation did not significantly occur during lyophilization.

Similar T_g measurements were carried out for lyophilized insulin alone, trehalose alone, and dextran alone samples preequilibrated at 12% RH.

Determination of $T_{1\rho}$ of Insulin Carbonyl Carbon by ^{13}C Solid-State NMR

The $T_{1\rho}$ of insulin carbonyl carbon in lyophilized insulin, insulin–dextran, and insulin–trehalose samples was determined at 25°C using a UNITY plus spectrometer operating at a proton resonance frequency of 400 MHz (Varian Inc., Palo Alto, CA, USA). Lyophilized samples were preequilibrated at 12% RH. Spin-locking field was equivalent to 19 kHz as a result of amplifier timing out. The rotor size was 7 mm and spinning speed was 4 kHz. Peak height at approximately 180 ppm attributed to insulin carbonyl carbon was followed with delay times of 1, 5, 10, 20, 30, 50, and 80 ms.

Similar measurements of $T_{1\rho}$ were performed for lyophilized PGA alone, PGA–dextran, and PGA–trehalose samples. Signal decay was determined from the area of a slightly split peak around approximately 180 ppm attributed to PGA carbonyl carbon in the backbone and carboxylic carbon in the side chain.

Water Vapor Absorption

Water vapor absorption isotherms of lyophilized insulin alone, dextran alone, trehalose alone, insulin–trehalose, and insulin–dextran samples were measured gravimetrically at 25°C using an automated vacuum electrobalance (Model MB-300G, VTI Corp., Hialeah, FL, USA). Samples were dried under vacuum until changes in weight were less than 1 μg per 10 min. Water contents of the samples at partial vapor pressures of 0.10 and 0.20 were determined based on equilibrated sample weight (changes in weight of less than 1 μg per 10 min).

Determination of Insulin Degradation Rate in Lyophilized Formulations Containing Dextran

Lyophilized insulin–dextran samples with various T_g values in tubes with a tight screw cap were stored at a constant temperature (40–90°C), removed at various times, and stored in liquid nitrogen until assayed. Samples were dissolved in 1.5 mL of 0.01 M $(NH_4)_2SO_4$ (pH 2.2, adjusted with concentrated H_2SO_4) and subjected to reverse-phase high-performance liquid chromatography (HPLC), as reported (10). The column used was Inertsil WP-300 (C8, 4.6 mm × 250 mm, GL Sciences Inc., Tokyo, Japan) maintained at 35°C. Elutions were performed using a mixture of 0.01 M $(NH_4)_2SO_4$ (pH 2.2) and acetonitrile solution of 0.07%(v/v) trifluoroacetic acid (72.5:27.5) for 1 min. The ratio of the acetonitrile solution increased linearly from 27.5 to 30% in 15 min and from 30 to 35% in 22 min. The detection wavelength was 214 nm.

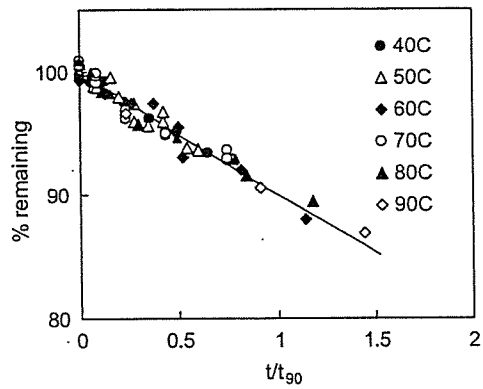

Fig. 1. Time courses of insulin degradation in lyophilized formulation containing dextran at 12% relative humidity (RH) at various temperatures. Time is scaled to the t_{90} for each temperature.

RESULTS

Insulin Degradation in Lyophilized Formulation Containing Dextran

A21-desamido insulin and insulin dimer were detected by HPLC and size-exclusion chromatography, respectively, as degradation products of lyophilized insulin formulations containing dextran, thus suggesting that the major degradation pathways are A21-desamido insulin formation and dimerization via the cyclic anhydride intermediate, as reported for lyophilized insulin–trehalose and insulin–poly(vinylpyrrolidone) systems (12). The same degradation mechanism has been observed for insulin in acidic solution (14) and in lyophilized solids derived from acidic solutions (15). Figure 1 shows the time courses of insulin degradation at 12% RH in lyophilized formulations containing dextran. Similar time courses were also obtained at 43 and 60% RH. The time courses of insulin degradation determined by HPLC correspond to the formation of the cyclic anhydride intermediate as a rate-determining step. The line shown in Fig. 1 represents the theoretical curve for first-order kinetics. Degradation at initial stages was describable with first-order kinetics under all the temperature and humidity conditions examined. The time required for 10% degradation (t_{90}) was calculated from the apparent first-order rate constant.

Figure 2 shows the temperature dependence of the calculated t_{90} for the insulin–dextran system. Solid lines in the figure represent the regression curves obtained by curve fitting according to Eq. (1).

$$k' = k\left(\frac{\alpha' D_r}{k + \alpha' D_r}\right) = k\left(\frac{\alpha T\left(\frac{1}{\tau}\right)^{\xi}}{k + \alpha T\left(\frac{1}{\tau}\right)^{\xi}}\right) = \frac{-\ln(0.9)}{t_{90}} \quad (1)$$

where k' is the rate constant for a reaction in which the rate-determining step involves molecular diffusion (16). k is the rate constant for conditions under which reactants have high diffusibility, such that k may be described by Eq. (2) using the activation energy (ΔH), frequency factor (A), and gas constant (R).

$$k = A\ exp\left(\frac{-\Delta H}{RT}\right) \quad (2)$$

D_r is the diffusion coefficient of the reactant and α (α') is a constant representing the correlation between D_r and reaction rate. D_r was assumed to be related to the structural relaxation time (τ) according to Eq. (3),

$$\frac{D_{r2}}{D_{r1}} \approx \left(\frac{T_2}{T_1}\right)\left(\frac{\tau_1}{\tau_2}\right)^{\xi} \quad (3)$$

where ξ is a constant that represents the degree of decoupling between D_r and τ (2). Equation (1) explains that the reaction rate is diffusion-controlled when $k \gg \alpha' D_r$ ($k' = \alpha' D_r$), whereas the reaction rate is controlled by the kinetics of the reaction when $\alpha' D \gg k$ ($k' = k$). The temperature dependence of k' changes around T_g when the reaction rate is diffusion-controlled, but not when the reaction rate is controlled by the kinetics of the reaction. The slope of the regression

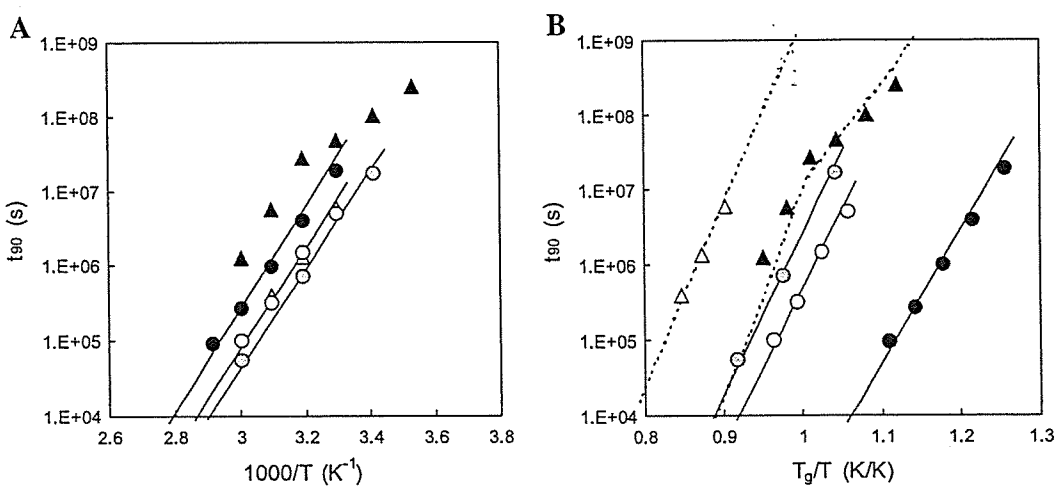

Fig. 2. Temperature dependence (A) and T_g dependence (B) of t_{90} for insulin degradation in lyophilized formulation containing dextran or trehalose. ●, dextran 12% RH; ○, dextran 43% RH; ⊙, dextran 60% RH; ▲, trehalose 12% RH; △, trehalose 43% RH. t_{90} values represent the average of two measurements.

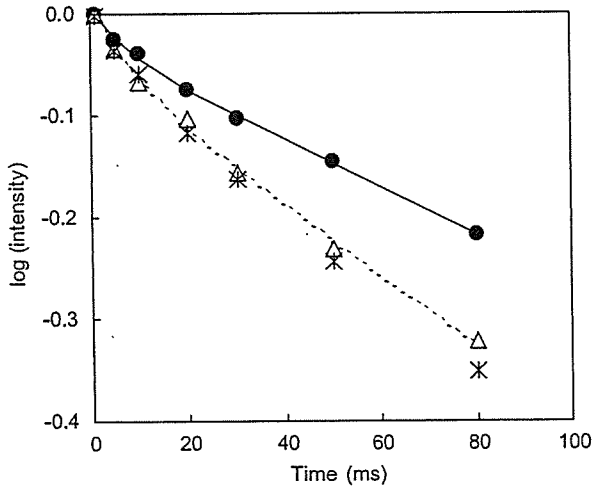

Fig. 3. Time courses of rotating-frame spin-lattice relaxation for insulin carbonyl carbon in lyophilized insulin (△), insulin–dextran (*), and insulin–trehalose (•) systems. 25°C, 12% RH.

curves shown in Fig. 2 did not show significant changes around T_g. Therefore, k'/k is considered unity, indicating that the reaction is reaction-controlled. Furthermore, the t_{90} *vs.* T_g/T plots for different humidity conditions did not converge around T_g. Curve fitting provided ΔH estimates of 31.2, 30.5, and 30.0 kcal/mol for 12, 43, and 60% RH, respectively.

Figure 2 also shows the temperature dependence of t_{90} for the insulin–trehalose system reported previously (10) for comparison. As shown in Fig. 2A, t_{90} for the insulin–dextran system at a given temperature was approximately one order of magnitude shorter than that for the insulin–trehalose system at 12% RH, whereas no significant difference in t_{90} was observed between the two systems at 43% RH. Comparison of the t_{90} obtained at 12% RH in the temperature range below the T_g indicates that the insulin–dextran system exhibited a substantially smaller t_{90} value at a given T_g/T than the insulin–trehalose system, as shown in Fig. 2B.

$T_{1\rho}$ of Insulin Carbonyl Carbon

Figure 3 shows the time courses for the spin-lattice relaxation of insulin carbonyl carbon in lyophilized insulin alone, as well as in lyophilized insulin–dextran and insulin–trehalose systems, observed at 25°C and 12% RH. Spin-lattice relaxation was not significantly affected by the presence of dextran, but it was significantly retarded by the presence of trehalose.

The time course of spin-lattice relaxation was describable with a biexponential equation including two different $T_{1\rho}$ values. Figure 4A and B shows the longer $T_{1\rho}$ estimate and the proportion of the shorter $T_{1\rho}$, respectively, calculated by curve fitting, with the shorter $T_{1\rho}$ being 8 ms. The proportion of the shorter $T_{1\rho}$ was approximately 0.1 regardless of the presence of dextran or trehalose. The longer $T_{1\rho}$ of the dominating proportion, probably attributed to carbonyl carbons in the backbone, was substantially elevated by the presence of trehalose. Under the conditions examined here (slow motional regime), $T_{1\rho}$ is proportional to the correlation time that corresponds to the β-relaxation time (11). Therefore, the increase in the longer $T_{1\rho}$ caused by trehalose suggests that the mobility of carbonyl carbons in the backbone of the insulin molecule is inhibited by trehalose.

To examine the generality of the effects of trehalose and dextran on the $T_{1\rho}$ of carbonyl carbon, $T_{1\rho}$ was measured for PGA carbonyl carbons in lyophilized PGA–trehalose and PGA–dextran systems. The longer $T_{1\rho}$ was substantially increased by the presence of trehalose in a similar manner as the $T_{1\rho}$ of insulin carbonyl carbons. The proportions of the shorter $T_{1\rho}$, probably attributed to carbonyl carbons in the side chains, were estimated to be approximately 0.1 and 0.2 for the insulin–trehalose and PGA–trehalose systems, respectively. In contrast, the proportions of carbonyl carbons present in the side chains are calculated to be 0.09 and 0.5 for insulin and PGA, respectively. This finding suggests that a portion of the carbonyl carbons in the side chain of PGA exhibits low mobility comparable to the carbonyl carbons in the backbone of the molecule.

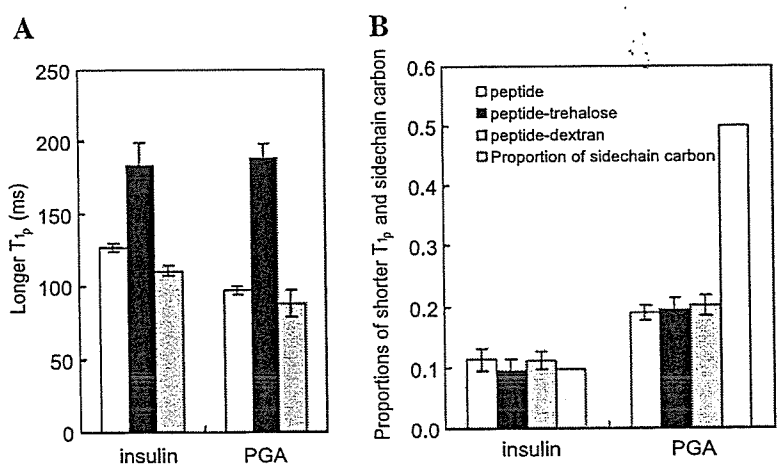

Fig. 4. Effect of trehalose and dextran on the $(T_{1\rho})$ of insulin and poly-L-glutamic acid carbonyl carbons. Signal decay was analyzed by a biexponential equation. The longer $(T_{1\rho})$ and the proportion of shorter $(T_{1\rho})$ are shown in (A) and (B), respectively. (B) also shows the proportion of carbons in the side chain.

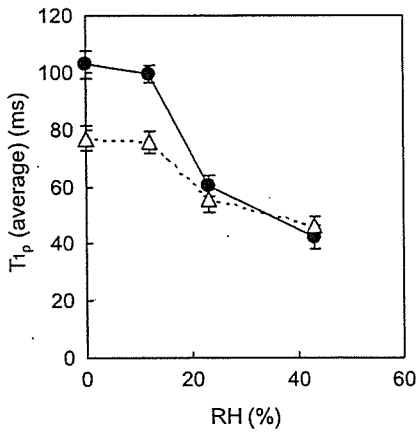

Fig. 5. Effect of humidity on the $(T_{1\rho})$ of insulin carbonyl carbon in the backbone carbon in lyophilized insulin (△) and insulin–trehalose (•) systems. 25°C. Bars represent standard deviation (n = 3).

Figure 5 shows the effects of humidity on the longer $T_{1\rho}$ of insulin carbonyl carbons. The prolongation of $T_{1\rho}$ brought about by the addition of trehalose was eliminated at above 23% RH, suggesting that trehalose inhibits the mobility of insulin carbonyl carbons in the backbone only under low humidity conditions.

In an effort to elucidate the relationship between the changes in $T_{1\rho}$ and in matrix T_g associated with the addition of excipients, the amount of absorbed water at 10 and 20% RH as well as matrix T_g at 12% RH were measured for the lyophilized insulin alone, trehalose alone, dextran alone, insulin–trehalose, and insulin–dextran systems, and the results are shown in Table I. The insulin–dextran system exhibited a similar amount of absorbed water as dextran alone and exhibited an intermediate T_g value between those of insulin alone and dextran alone. Meanwhile, the insulin–trehalose system exhibited a larger amount of absorbed water and a lower T_g than insulin alone and trehalose alone. These findings indicate that the addition of trehalose increases water absorption, resulting in decreased matrix T_g.

DISCUSSION

Our previous study demonstrated that the degradation rate of insulin in a lyophilized insulin–trehalose system is significantly affected by matrix T_g under low humidity conditions, but not under higher humidity conditions, based on curve fitting for the temperature dependence of t_{90} according to Eq. (1) (dotted lines in Fig. 2B). The present study demonstrated that the temperature dependence of t_{90} for a lyophilized insulin–dextran system did not exhibit significant changes in the slope of the regression curve around the T_g, even under low humidity conditions. The t_{90} of insulin degradation in the insulin–trehalose system was approximately one order of magnitude greater than that in the insulin–dextran system at 12% RH, but the difference was not significant at 43% RH (Fig. 2A). Although dextran was expected to stabilize insulin because of the high T_g value (matrix T_g of the insulin–dextran and insulin–trehalose systems at 12% RH was 107 and 44°C, respectively), the insulin–dextran system exhibited a substantially shorter t_{90} than the insulin–trehalose system at a given T_g/T (matrix mobility) (Fig. 2B). This finding suggests that it is not matrix mobility that determines the stability of insulin. This notion is supported by the finding that the temperature dependence of t_{90} for the insulin–dextran systems with a different T_g caused by a different water content did not converge around T_g as expected when matrix mobility is a determinant of degradation rate.

Other than the matrix mobility of amorphous solids, another motion suggested to determine the stability of the solids is β-relaxation, a smaller-scale motion than matrix mobility (9). It is widely known that $T_{1\rho}$ can effectively detect molecular motions on the timescale of 10^{-5} s and reflect the β-relaxation of molecules in amorphous solids (11,17,18). The present study demonstrated that the $T_{1\rho}$ of insulin carbonyl carbons under low humidity conditions was substantially increased by the presence of trehalose, but not by the presence of dextran (Fig. 4). This increase in $T_{1\rho}$ indicates that trehalose retards the β-relaxation of insulin. No effect of dextran on the $T_{1\rho}$ suggests that miscibility between insulin and dextran is lower than that between insulin and trehalose. Meanwhile, the addition of trehalose brought about a decrease in T_g or an increase in matrix mobility (Table I). The behaviors of $T_{1\rho}$ and T_g described above suggest that the β-relaxation of insulin molecules rather than the matrix mobility is inhibited by trehalose. The addition of trehalose improved the stability of insulin and inhibited the β-relaxation of insulin under low humidity conditions, whereas the addition of dextran did not exhibit significant effects on the stability nor on the β-relaxation (Figs. 2 and 4). Therefore, the β-relaxation of insulin rather than the matrix mobility seems to be closely related to the stability of insulin. Close correlations between β-relaxation and stability are also suggested by the findings that the β-relaxation-inhibiting effects of trehalose were eliminated at above 23% RH (Fig. 5) and that the stabilizing effect of trehalose was eliminated at 43% RH (Fig. 2A). The β-relaxation-inhibiting effect of trehalose may be attributed to the ability of trehalose to interact with insulin through hydrogen bonding. It is well known that sugars such as trehalose improve the storage stability of lyophilized protein formulations regardless of their relatively low T_g values (1). This stabilizing effect is generally attributed to interaction between sugar and protein.

The degradation rate of insulin under low humidity conditions was significantly affected by matrix T_g in lyophilized insulin–trehalose systems, as reported previously (10), but was not significantly affected by matrix T_g in the insulin–dextran systems. These findings suggest that the β-

Table I. Effect of Trehalose and Dextran on Water Content and T_g

	Water content (%/solid)		
	10% RH	20% RH	T_g at 12% RH
Insulin	2.8 ± 0.1	3.6 ± 0.1	106 ± 2
Trehalose	3.3 ± 0.0	4.8 ± 0.0	66 ± 1
Dextran	5.5 ± 0.5	7.6 ± 0.7	131 ± 4
Insulin–trehalose	4.3 ± 0.1	6.5 ± 0.0	48 ± 3
Insulin–dextran	5.6 ± 0.2	7.8 ± 0.2	107 ± 3

SD (n = 3).
RH = relative humidity.

relaxation of insulin is inhibited by trehalose and, thus, becomes a rate determinant, while it is not inhibited by dextran, and the chemical activational barrier (activation energy) becomes the major rate determinant.

D_r in Eq. (1) is related to the structural relaxation time (τ), which reflects matrix mobility, according to Eq. (3). Therefore, it was previously concluded that the degradation rate of insulin at low humidities in the insulin–trehalose system is affected by matrix mobility. However, it may also be possible that β-relaxation time is a determinant of degradation rate, such that τ in Eq. (1) represents β-relaxation time. The temperature dependence of the degradation rate at low humidities, which exhibits a change in slope around T_g, can be explained by assuming that β-relaxation is coupled with matrix mobility. It is generally understood that smaller-scale motions can be coupled with matrix mobility (5,18,19). The thought that β-relaxation rather than matrix mobility determines the degradation rate is reasonable because insulin degradation via a cyclic intermediate is not believed to require large-scale motions, such as matrix mobility (5).

CONCLUSION

The storage stability and β-relaxation of insulin lyophilized with trehalose were compared with those of insulin lyophilized with dextran. The addition of trehalose improved the stability of insulin and inhibited the β-relaxation of insulin under low humidity conditions, while the addition of dextran did not exhibit significant effects on stability nor on β-relaxation. The β-relaxation-inhibiting and the stabilizing effects of trehalose were eliminated at higher humidities. These results suggest that β-relaxation of insulin is inhibited by trehalose at low humidity, presumably as a result of insulin–trehalose interaction, and thus, β-relaxation is a determinant of the degradation rate of insulin. In contrast, the β-relaxation of insulin is not inhibited by dextran, and thus, the chemical activational barrier (activation energy) is the major rate determinant. The molecular motion related to the stability of insulin in the present glassy systems seems to be the β-relaxation of insulin rather than the matrix mobility.

REFERENCES

1. M. J. Pikal. Chemistry in solid amorphous matrices: implication for biostabilization. In H. Levine (ed.). *Amorphous Food and Pharmaceutical Systems*, Royal Society of Chemistry, Cambridge, UK, 2002, pp. 257–272.
2. Y. Guo, S. R. Byrn, and G. Zografi. Physical characteristics and chemical degradation of amorphous quinapril hydrochloride. *J. Pharm. Sci.* **89**:128–143 (2000).
3. S. Yoshioka, Y. Aso, and S. Kojima. Temperature- and glass transition temperature-dependence of bimolecular reaction rates in lyophilized formulations described by the Adam-Gibbs-Vogel equation. *J. Pharm. Sci.* **93**:1062–1069 (2004).
4. S. P. Duddu, G. Zhang, and P. R. Dal Monte. The relationship between protein aggregation and molecular mobility below the glass transition temperature of lyophilized formulations containing a monoclonal antibody. *Pharm. Res.* **14**:596–600 (1997).
5. M. J. Pikal. Mechanisms of protein stabilization during freeze-drying and storage: The relative importance of thermodynamic stabilization and glassy state relaxation dynamics. L. Rey and J. C. May (eds.). *Freeze-Drying/Lyophilization of Pharmaceutical and Biological Products*, Marcel Dekker, New York, 2004, pp. 63–107.
6. S. Rossi, M. P. Buera, S. Moreno, and J. Chirife. Stabilization of the restriction enzyme *Eco*RI dried with trehalose and other selected glass-forming solutes. *Biotechnol. Prog.* **13**:609–616 (1997).
7. C. Schebor, L. Burin, M. P. Buera, J. M. Aguilera, and J. Chirife. Glassy state and thermal inactivation of invertase and lactase in dried amorphous matrices. *Biotechnol. Prog.* **13**:857–863 (1997).
8. Y. Chen, J. L. Aull, and L. N. Bell. Invertase storage stability and sucrose hydrolysis in solids as affected by water activity and glass transition. *J. Agric. Food Chem.* **47**:504–509 (1999).
9. T. R. Noel, R. Parker, and S. G. Ring. Effect of molecular structure and water content on the dielectric relaxation behaviour of amorphous low molecular weight carbohydrates above and below their glass transition. *Carbohydr. Res.* **329**:839–845 (2000).
10. S. Yoshioka and Y. Aso. A quantitative assessment of the significance of molecular mobility as a determinant for the stability of lyophilized insulin formulations. *Pharm. Res.* **22**:1358–1364 (2005).
11. T. C. Farrar and E. D. Becker. *Pulse and Fourier Transform NMR, Introduction to Theory and Methods*, Academic, New York, 1971.
12. R. T. Darrington and B. D. Anderson. The role of intramolecular nucleophilic catalysis and the effects of self-association on the deamidation of human insulin at low pH. *Pharm. Res.* **11**: 784–793 (1994).
13. S. Yoshioka and Y. Aso. Negligible contribution of molecular mobility to the degradation rate of insulin lyophilized with poly(vinylpyrrolidone). *J. Pharm. Sci.* (2006), in press.
14. R. T. Darrington and B. D. Anderson. Effect of insulin concentration and self-association on the partitioning of its A-21 cyclic anhydride intermediate to desamido insulin and covalent dimer. *Pharm. Res.* **12**:1077–1084 (1995).
15. R. G. Strickley and B. D. Anderson. Solid-state stability of human insulin. II. Effect of water on reactive intermediate partitioning in lyophiles from pH 2–5 solutions: stabilization against covalent dimer formation. *J. Pharm. Sci.* **86**:645–653 (1997).
16. M. Karel and I. Saguy. Effects of water on diffusion in food systems. *Adv. Exp. Med. Biol.* **302**:157–173 (1991).
17. G. R. Moran, K. R. Jeffrey, J. M. Thomas, and J. R. Stevens. A dielectric analysis of liquid and glassy solid glucose/water solutions. *Carbohydr. Res.* **328**:573–584 (2000).
18. S. Yoshioka and Y. Aso. Glass transition-related changes in moecular mobility below glass transition temperature of freeze-dried formulations, as measured by dielectric spectroscopy and solid state nuclear magnetic resonance. *J. Pharm. Sci.* **94**:275–287 (2005).
19. S. Yoshioka, Y. Aso, S. Kojima, S. Sakurai, T. Fujiwara, and H. Akutsu. Molecular mobility of protein in lyophilized formulations linked to the molecular mobility of polymer excipients, as determined by high resolution 13C solid-state NMR. *Pharm. Res.* **16**:1621–1625 (1999).

Physical Stability of Amorphous Acetanilide Derivatives Improved by Polymer Excipients

Tamaki MIYAZAKI,* Sumie YOSHIOKA, and Yukio ASO

Division of Drugs, National Institute of Health Sciences; 1–18–1 Kamiyoga, Setagaya-ku, Tokyo 158–8501, Japan.
Received February 15, 2006; accepted May 18, 2006; published online May 25, 2006

Crystallization rates of drug-polymer solid dispersions prepared with acetaminophen (ACA) and *p*-aminoacetanilide (AAA) as model drugs, and polyvinylpyrrolidone and polyacrylic acid (PAA) as model polymers were measured in order to further examine the significance of drug–polymer interactions. The crystallization of AAA and ACA was inhibited by mixing those polymers. The most effective inhibition was observed with solid dispersions of AAA and PAA. The combination of AAA and PAA showed a markedly longer enthalpy relaxation time relative to drug alone as well as a higher T_g than predicted by the Gordon–Taylor equation, indicating the existence of a strong interaction between the two components. These observations suggest that crystallization is effectively inhibited by combinations of drug and polymer that show a strong intermolecular interaction due to proton transfer between acidic and basic functional groups.

Key words crystallization rate; solid dispersion; drug–polymer interaction; enthalpy relaxation; glass transition temperature

Preparation of amorphous forms of poorly water-soluble pharmaceuticals is one of the most effective methods to improve their solubility. However, amorphous solids are physically unstable, and crystallization during storage presents a problem. It is known that crystallization can be inhibited by increasing the glass transition temperature (T_g) of the solid dispersion by addition of a polymer excipient with a high T_g. Decreases in crystallization rates with increasing T_g have been demonstrated for several systems.[1—3] Nevertheless, stabilizing effects that could not be explained only by an increase in T_g have been reported. The crystallizations of amorphous sucrose[4] and indomethacin[5] were effectively inhibited in solid dispersions with a small amount of polymer (<10%) that exhibited no significant increase in T_g. In our previous report concerning the crystallization of amorphous acetaminophen (ACA) in solid dispersions with 10% polyacrylic acid (PAA) or polyvinylpyrrolidone (PVP), the crystallization rate in the temperature range 45—60 °C was slower in ACA–PAA dispersions than in ACA–PVP dispersions with a similar T_g.[6] These results indicate that other factors in addition to T_g can influence the crystallization rate. Drug–polymer interactions such as hydrogen bonding may decrease crystallization rates, as indicated by infrared[2,5,7] and Fourier transform Raman[8,9] spectroscopy and nuclear magnetic resonance relaxation[10] measurements. In solid dispersions with PVP, the carbonyl group is believed to participate in the interaction.[2,5,7—10] The participation of carboxyl group of PAA in salt forming with basic drugs have also been reported.[11,12]

The purpose of this study was to further examine the significance of interactions to the physical stability of solid dispersions. The isothermal crystallization behavior was investigated using various solid dispersions prepared with ACA and *p*-aminoacetanilide (AAA) as model drugs. They have acetanilide moiety in common and an opposite polar group at the para position: hydroxyl group (ACA) and amino group (AAA). For polymers, PAA with a carboxyl group and PVP with a carbonyl group were selected. PVP only acts as proton acceptor, while PAA acts as both a proton donor and an acceptor. Besides the crystallization rate, the enthalpy relaxation time and the T_g were measured as indicators of drug–polymer interaction. The role of salt forming in stabilizing amorphous solids was compared with that of hydrogen bonding.

Experimental

Materials ACA, AAA and PVP (average molecular weight (M_w) of 360000) were obtained from Sigma Chemical Co. PAA (M_w 5000) was obtained from Wako Pure Chemical Industries Ltd.

Preparation of Amorphous Drugs and Drug–Polymer Solid Dispersions Amorphous ACA and AAA were prepared by melt quenching in a cell of a differential scanning calorimeter (DSC2920, TA Instruments) with a dry nitrogen gas purge at 20 ml/min. Crystalline drug (2—3 mg) was put in an aluminum pan and sealed with a pierced lid. The pan was heated to 182 °C at a heating rate of 20 °C/min, kept at that temperature for 3 min, and cooled to −80 °C for ACA and −90 °C for AAA at a cooling rate of 40 °C/min by pouring liquid nitrogen into the cooling jacket surrounding the cell. And then it was reheated to room temperature at a heating rate of 20 °C/min. The temperatures of −80 °C and −90 °C corresponded to the temperature 100 °C below the T_g for ACA and AAA, respectively.

Drug–polymer solid dispersions and polymer-alone samples were prepared by freeze-drying. Aqueous solutions of an acetanilide derivative and a polymer at the desired mixing ratio were frozen in polypropylene vessels by immersion in liquid nitrogen for 10 min and were then dried at a vacuum level of <5 Pa for 24 h in a lyophilizer (Freezvac 1CFS, Tozai Tsusho Co.). The shelf temperature was −40 °C for the first hour, 20 °C for the subsequent 19 h, and 35 °C for the rest of the period to complete the dehydration. The obtained mixtures or polymer cakes (2—3 mg) were put in an aluminum pan and sealed with a pierced lid. The pan was heated to approximately 20 °C above the T_g at a heating rate of 20 °C/min, then cooled to approximately 100 °C below the T_g at a cooling rate of 40 °C/min and reheated to room temperature at a heating rate of 20 °C/min, in order to give the same thermal history and to remove residual water from samples. No endothermic peak resulting from evaporation of water was observed in the second heating run. Since mixtures containing more than 50% ACA or AAA crystallized during the freeze-drying or during heating in the DSC cell, samples were heated to more than 10 °C above the end of melting endothermic event, kept at that temperature for 3 min, and rapidly cooled to approximately 100 °C below the T_g. And then it was reheated to room temperature at a heating rate of 20 °C/min.

Measurement of Isothermal Crystallization Rate The isothermal crystallization rate was measured with pure drugs and solid dispersions containing 2—10% polymer. The samples were stored at a constant temperature in desiccators containing P_2O_5. After various periods of time, change in heat capacity (ΔC_p) at T_g was measured by DSC with a heating rate of 20 °C/min. The ratio of amorphous form remaining at time t, $x(t)$, was calculated according to Eq. 1:

$$x(t)=\Delta C_p/\Delta C_{p0} \quad (1)$$

* To whom correspondence should be addressed. e-mail: miyazaki@nihs.go.jp

where ΔC_{pt} and ΔC_{p0} are the changes in ΔC_p at time t and initially, respectively. The decrease in $x(t)$ as a function of storage time was analyzed according to the Avrami equation (Eq. 2) with a n value of 3, to calculate the time required for 10% of the amorphous solid to crystallize (t_{90}):

$$x(t)=\exp(-kt^n) \quad (2)$$

where k is the crystallization rate constant and n is the Avrami index related to the nucleation mechanism and the dimensionality of the growth process.

Measurement of Enthalpy Relaxation The samples were stored at a constant temperature (10—35 °C below the T_g). Storage was performed in desiccators containing P_2O_5 putting in water baths or air baths for temperatures under 90 °C, and was performed in the DSC cell for temperatures above 90 °C.

After various periods of time, the samples were cooled to approximately 100 °C below the T_g and heated (20 °C/min) through their T_g to measure endothermic recovery by DSC. The fraction of glass relaxed at time t, $\phi(t)$, was calculated by Eq. 3:

$$\phi(t)=\Delta H_t/\Delta H_\infty \quad (3)$$

where ΔH_t is the enthalpy recovery at time t and ΔH_∞ is the maximum enthalpy recovery calculated from T, T_g and ΔC_p according to Eq. 4:

$$\Delta H_\infty=\Delta C_p(T_g-T) \quad (4)$$

The T_g and ΔC_p values observed for the sample before storage were used to calculate the ΔH_∞ value. The enthalpy relaxation time (τ) was calculated according to the Kohlrausch–Williams–Watts (KWW) equation (Eq. 5):

$$1-\phi(t)=\exp[(-t/\tau)^\beta] \quad (5)$$

where β is a parameter representing distribution of the relaxation time. No crystallization was observed during the enthalpy relaxation measurements.

Measurement of T_g and Prediction of T_g from the Gordon–Taylor Equation T_g measurements of amorphous drugs and drug–polymer solid dispersions were performed by DSC with a dry nitrogen gas purge at 20 ml/min. Indium was used to calibrate the cell constant and the temperature of the instrument. Samples were heated at a rate of 20 °C/min and the values of ΔC_p and T_g at the inflection point were obtained.

The T_g values of the amorphous solid dispersions were predicted with the Gordon–Taylor equation, which assumes that the two components are ideally mixed[13]:

$$T_{g12}=(w_1T_{g1}+Kw_2T_{g2})/(w_1+Kw_2) \quad (6)$$

where w_1 and w_2 are the mass fractions of each component and T_{g1} and T_{g2} are the glass transition temperatures of each component. The constant K is related to the free volume of the two components and can be calculated by the Simha–Boyer rule:

$$K=T_{g1}\rho_1/T_{g2}\rho_2 \quad (7)$$

where ρ_1 and ρ_2 are the densities of each component. Density values were measured by helium pycnometry (AccuPyc 1330, Shimadzu Co.) at ambient temperature. Amorphous ACA and AAA were prepared by melting the crystalline form in Teflon vessels at 180 °C for 10 min followed by quench cooling by immersion into liquid nitrogen. Amorphous polymers were freeze-dried samples. Table 1 shows the T_g and density values of the drugs and polymers in the amorphous state.

Table 1. T_g and Density Values of Drugs and Polymers

Sample	T_g (°C)	Density (g/cm^3)
ACA	25.1±0.6	1.23±0.003
AAA	9.5±0.4	1.19±0.001
PAA	117.6±0.5	1.40±0.002
PVP	181.6±0.5	1.20±0.000

Values are mean±S.D. (n>3).

Table 2. T_g (°C) Values of Amorphous Drugs and Solid Dispersions

Polymer content (%)	ACA		AAA	
	PAA	PVP	PAA	PVP
0	25.1±0.6		9.5±0.4	
2	26.2±0.4	25.6±0.2	12.9±0.5	13.0±0.1
5	26.8±0.6	—	15.3±0.3	14.1±0.2
10	29.3±0.4	27.8±0.3	19.7±0.7	16.4±0.3

Values are mean±S.D. (n>3).

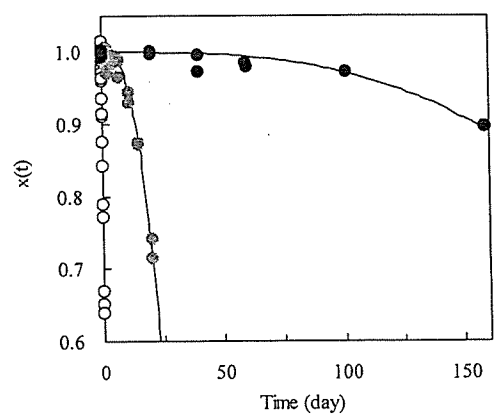

Fig. 1. Ratio of Amorphous form Remaining in AAA and AAA–PAA Solid Dispersions at 15 °C

○: drug alone, ●: 2%PAA, ●: 5%PAA. Solid lines denote the fitting to the Avrami equation.

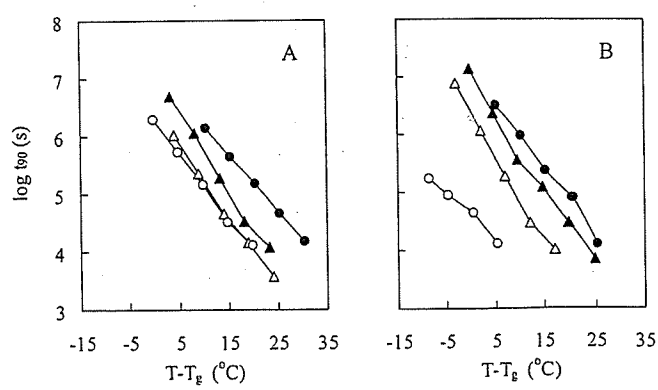

Fig. 2. Effect of PAA on the t_{90} for Crystallization of ACA (A) and AAA (B) at Various Storage Temperatures

○: without PAA, △: 2%PAA, ▲: 5%PAA, ●: 10%PAA.

Results

Isothermal Crystallization of Drug–Polymer Solid Dispersions A small amount of polymer somewhat increased the T_g of amorphous ACA and AAA (Table 2). Figure 1 shows typical time profiles of AAA crystallization in amorphous AAA and amorphous AAA–PAA solid dispersions at 15 °C as measured by the decrease in ΔC_p. Increasing amounts of PAA progressively retarded the crystallization. The t_{90} were calculated by fitting the data showing $x(t)$>0.6. Figures 2A and B show the effect of PAA on the t_{90} for crystallization of ACA and AAA in the solid dispersions at various storage temperatures (T). Compared at the same ($T-T_g$), the t_{90} increased with increasing amounts of PAA in both ACA–PAA and AAA–PAA solid dispersions. Especially for AAA, 2% PAA increased the t_{90} by more than one order of magnitude relative to that of pure AAA. Figure 3 shows the effect of polymer species on the t_{90}. Figure 3A also shows the previously reported results for 10% polyacrylic acid with M_w

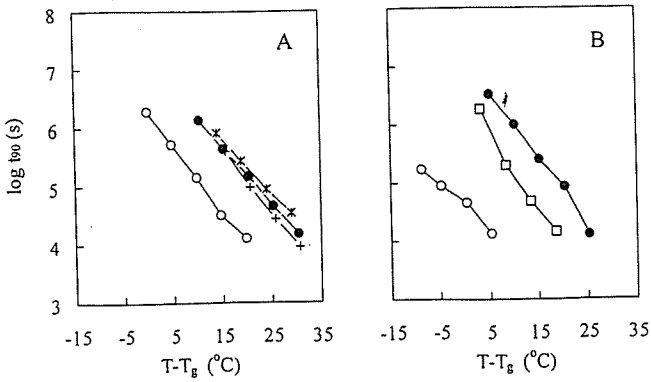

Fig. 3. Effect of Polymers on the t_{90} for Crystallization of ACA (A) and AAA (B) at Various Storage Temperatures

(A) ○: ACA, ●: ACA-PAA, *: ACA with polyacrylic acid (M_w of 25000)*, +: ACA with polyvinylpyrrolidone (M_w of 40000)*. (B) ○: AAA, ●: AAA–PAA, □: AAA–PVP. The mixing ratio of drug–polymer solid dispersions was 90 : 10. * The data were taken from ref. 6.

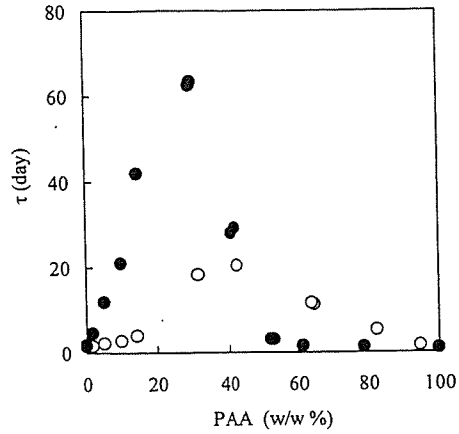

Fig. 5. Relationship between PAA Content and τ of ACA–PAA (○) and AAA–PAA (●)

Samples were stored at 20 °C below the T_g.

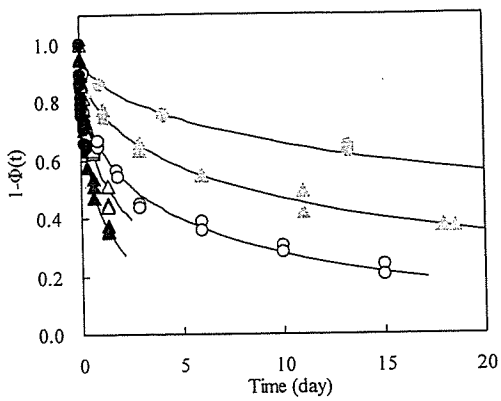

Fig. 4. Enthalpy Relaxation Behavior of Amorphous Samples

▲: ACA at 5 °C, ▲: ACA–PAA (70 : 30) at 25 °C, △: ACA–PVP (90 : 10) at 10 °C. ●: AAA at −10 °C, ●: AAA–PAA (70 : 30) at 30 °C, ○: AAA–PVP (90 : 10) at −3 °C. The lines denote the fitting to the KWW equation.

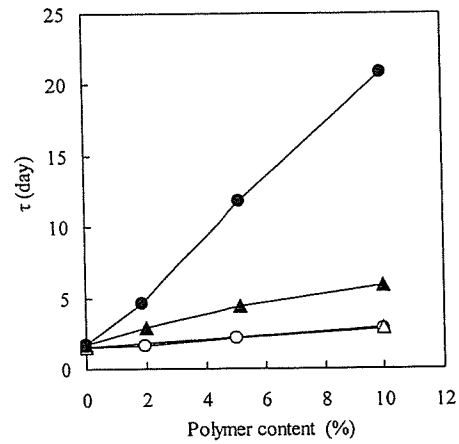

Fig. 6. Changes in τ of Solid Dispersions with Increasing Polymer Content

○: ACA–PAA, △: ACA–PVP, ●: AAA–PAA, ▲: AAA–PVP. Samples were stored at 20 °C below the T_g.

of 25000 and for 10% polyvinylpyrrolidone with M_w of 40000 (T_g: 31.3±0.5, 30.3±0.3 °C, respectively).[6] The inhibition effect of 10% polymer on the ACA crystallization rate was nearly the same irrespective of polymer species and the M_w. On the contrary for AAA, the t_{90} varied with polymers: PAA>PVP.

Enthalpy Relaxation of Amorphous Drug–Polymer Solid Dispersions Figure 4 shows typical profiles of the enthalpy relaxation behavior of drugs and drug–polymer solid dispersions at 20 °C below their T_g. All the enthalpy relaxation behaviors observed in this study could be analyzed according to the KWW equation with β between 0.46 and 0.48. Figure 5 shows the relationship between PAA content and τ of drug–PAA solid dispersions stored at 20 °C below their T_g. Maximum τ values were shown around 30—40% PAA, where the ratio of the number of drug molecules to the number of repeating unit (–CH(COOH)–CH_2–) in PAA chains was approximately 1 : 1. The maximum τ value of the AAA–PAA solid dispersions was approximately three times longer than that of the ACA–PAA dispersions.

Figure 6 illustrates the effect of small amount of polymer on τ. The τ of pure drug was similar for both ACA and AAA, and the increase in τ with PAA content was more marked in the AAA–PAA dispersions than in the ACA–PAA dispersions. The difference in τ-extending effect between PAA and PVP was not significant for ACA, however, it was apparent for AAA: PAA>PVP.

T_g of the Drug–Polymer Solid Dispersions A single T_g was observed for the ACA–polymer and AAA–polymer solid dispersions over the entire composition range. The T_g values obtained are plotted in Fig. 7. The lines in the figures represent predictions from the Gordon–Taylor equation. The AAA–PAA solid dispersions showed apparent positive deviation from the predicted values, whereas the T_g values of the ACA–PAA dispersions were in reasonable agreement with the predictions. The positive deviation was similar to those reported for the loperamide–PAA dispersions due to salt formation.[12] The T_g values of the drug–PVP dispersions tended to be lower than the prediction, as reported for sugar–PVP systems due to the overall loss in the number and strength of hydrogen bonds.[9]

Discussion

A single T_g was observed for all solid dispersions prepared with mixing the model drugs ACA or AAA, and the model polymers PAA or PVP, indicating a complete miscibility of

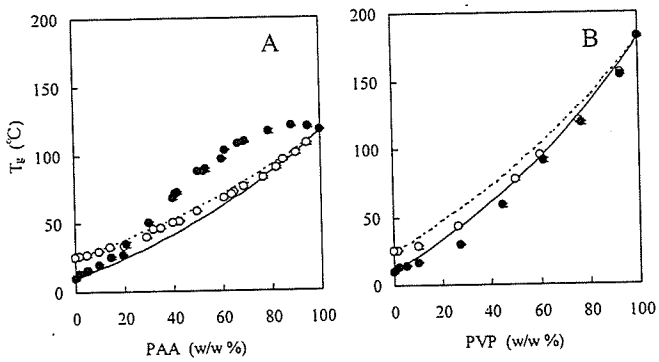

Fig. 7. T_g of Drug–PAA (A) and Drug–PVP (B) Solid Dispersions as a Function of Polymer Content

○: ACA, ●: AAA. The dotted and solid lines represent the prediction by the Gordon–Taylor equation for ACA and AAA, respectively. Each point represents the mean±S.D. (n>3).

the drug and polymer within the sensitivity limit of the DSC method. Thus, changes in matrix mobility may explain the retarded crystallization of ACA and AAA in the presence of PAA or PVP. The T_g of the solid dispersions increased with increasing polymer content. The increase in T_g caused by PAA was larger than that by PVP (Table 2). However, changes in matrix mobility can not completely explain the retarded crystallization, because the t_{90} values plotted against $(T-T_g)$ does not overlap each other (Fig. 2). Although the stabilizing effect of PAA for ACA crystallization was similar to that of PVP (Fig. 3A), PAA stabilized AAA to a greater extent than PVP (Fig. 3B). In addition, positive deviation in the T_g was observed for AAA–PAA dispersions (Fig. 7). This finding suggests that proton transfer occurred between AAA and PAA, as reported for basic drugs with PAA loperamide–PAA dispersions,[12] and resulted in the greater decrease in the crystallization rate of AAA. The interaction between the salt-forming components appeared to stabilize the amorphous state more effectively than the interaction through hydrogen bonding.

The stronger interaction between AAA and PAA was might also be confirmed by the enthalpy relaxation measurements. The AAA–PAA solid dispersions exhibited longer τ values than other dispersions in the range of 2—10% polymers (Fig. 6). This indicates that the molecular mobility of the AAA–PAA dispersion was reduced more intensely than others due to stronger interaction.

Conclusion

The crystallization of amorphous acetanilide derivatives was inhibited by mixing polymers having high T_g. The most effective inhibition was observed with solid dispersions of AAA and PAA. The combination of AAA and PAA showed a markedly longer τ relative to drug alone as well as a higher T_g than predicted by the Gordon–Taylor equation, indicating the existence of a strong interaction between the two components. These observations suggest that crystallization is effectively inhibited by combinations of drug and polymer that show a strong intermolecular interaction due to proton transfer between acidic and basic functional groups.

References

1) Yu L., *Adv. Drug Deliv. Rev.*, **48**, 27—42 (2001).
2) Khougaz K., Clas S. D., *J. Pharm. Sci.*, **89**, 1325—1334 (2000).
3) Zeng X. M., Martin G. P., Marriott C., *Int. J. Pharm.*, **218**, 63—73 (2001).
4) Shamblin S. L., Huang E. Y., Zografi G., *J. Thermal Anal.*, **47**, 1567—1579 (1996).
5) Matsumoto T., Zografi G., *Pharm. Res.*, **16**, 1722—1728 (1999).
6) Miyazaki T., Yoshioka S., Aso Y., Kojima S., *J. Pharm. Sci.*, **93**, 2710—2717 (2004).
7) Taylor L. S., Zografi G., *Pharm. Res.*, **14**, 1691—1698 (1997).
8) Taylor L. S., Zografi G., *J. Pharm. Sci.*, **87**, 1615—1621 (1998).
9) Shamblin S. L., Taylor L. S., Zografi G., *J. Pharm. Sci.*, **87**, 694—701 (1998).
10) Aso Y., Yoshioka S., *J. Pharm. Sci.*, **95**, 318—325 (2006).
11) Weuts I., Kempen D., Decorte A., Verreck G., Peeters J., Brewster M., Van den Mooter G., *Eur. J. Pharm. Sci.*, **22**, 375—385 (2004).
12) Weuts I., Kempen D., Verreck G., Peeters J., Brewster M., Blaton N., Van den Mooter G., *Eur. J. Pharm. Sci.*, **25**, 387—393 (2005).
13) Gordon M., Taylor J. S., *J. Appl. Chem.*, **2**, 493—500 (1952).

NOTE

Negligible Contribution of Molecular Mobility to the Degradation Rate of Insulin Lyophilized with Poly(vinylpyrrolidone)

SUMIE YOSHIOKA, YUKIO ASO, TAMAKI MIYAZAKI

National Institute of Health Sciences, 1-18-1 Kamiyoga, Setagaya-ku, Tokyo 158-8501, Japan

Received 1 January 2005; revised 15 April 2005; accepted 25 September 2005

Published online 21 February 2006 in Wiley InterScience (www.interscience.wiley.com). DOI 10.1002/jps.20504

ABSTRACT: The purpose of this study is to confirm the speculation which arose in our previous study that the degradation rate of insulin lyophilized with poly(vinylpyrrolidone) is mainly governed by the chemical activational barrier rather than molecular mobility. This speculation was based on the degradation data of insulin lyophilized with poly(vinylpyrrolidone) K-30 (PVP K-30), which was obtained at temperatures well below the glass transition temperature (T_g). In this study, the degradation rate of insulin at temperatures below and above T_g was determined using PVP 10k as an excipient, instead of PVP K-30, in order to examine whether or not the temperature dependence of the degradation rate changes around T_g. The relative contributions of molecular mobility and the activational barrier, calculated from the temperature- and T_g-dependence of the degradation rate, indicated that the contribution of molecular mobility to the degradation rate was negligible. Furthermore, the negligible contribution of molecular mobility was confirmed by the lack of significant change observed in the temperature- and T_g-dependence of the rate around T_g. © 2006 Wiley-Liss, Inc. and the American Pharmacists Association J Pharm Sci 95:939–943, 2006

Keywords: solid-state stability; glass transition; lyophilization; amorphous; physicochemical; molecular mobility; insulin

INTRODUCTION

An understanding of how the chemical stability of solid formulations is affected by molecular mobility is beneficial in the development and evaluation of stable solid dosage forms. We recently proposed an equation for quantitatively assessing the contribution of molecular mobility to the chemical reactivity of amorphous solids (Eq. 1),[1]

$$k' = k\left(\frac{\alpha' D_r}{k + \alpha' D_r}\right) = k\left(\frac{\alpha T\left(\frac{1}{\tau}\right)^{\xi}}{k + \alpha T\left(\frac{1}{\tau}\right)^{\xi}}\right) \quad (1)$$

where k' is the rate constant for a reaction in which the rate-determining step involves molecular diffusion.[2] k is the rate constant at the condition under which reactants have high diffusibility, such that k may be described by Eq. 2 using the activation energy (ΔH), the frequency factor (A) and the gas constant (R).

$$k = A \exp\left(\frac{-\Delta H}{RT}\right) \quad (2)$$

D_r is diffusion coefficient of the reactant and α (α') is a constant representing the correlation between D_r and reaction rate. D_r was assumed to relate to the structural relaxation time (τ) according to Eq. 3,

$$\frac{D_{r2}}{D_{r1}} \approx \left(\frac{T_2}{T_1}\right)\left(\frac{\tau_1}{\tau_2}\right)^{\xi} \quad (3)$$

Correspondence to: Sumie Yoshioka (Telephone: 81-3-3700-8547; Fax: 81-3-3707-6950; E-mail: yoshioka@nihs.go.jp)

Journal of Pharmaceutical Sciences, Vol. 95, 939–943 (2006)

where ξ is a constant that represents the degree of decoupling between D_r and τ.[3] k' in Eq. 1 can be converted to t_{90} (time required for 10% degradation) according to Eq. 4 for first-order degradation.

$$k' = \frac{-\ln(0.9)}{t_{90}} \quad (4)$$

Using Eq. 1, the relative contribution of molecular mobility and that of the chemical activational barrier, reflected in the activation energy, were calculated for the chemical degradation of insulin lyophilized with trehalose or poly(vinylpyrrolidone) K-30 (PVP K-30).[1] For the insulin-trehalose system, the ratio of the observed rate constant (k') to the rate constant governed only by the chemical activational barrier (k) at the glass transition temperature (T_g) was 0.05 at 12% relative humidity (RH). This ratio (k'/k) was greater than 0.9 at humidity levels between 23%RH and 60%RH, indicating that the significance of molecular mobility as a determinant for reactivity is greater at lower humidity. The insulin-PVP K-30 system, in contrast, exhibited a k'/k value greater than 0.95 even at 12%RH, suggesting that the significance of molecular mobility is small. This speculation was based on the degradation data obtained at temperatures well below T_g, but not on the observation that the temperature dependence of k' does not significantly change around T_g. This is because k' values around T_g could not be determined because of the high T_g of the insulin-PVP K-30 system.

In this study, the degradation rate of insulin lyophilized with PVP 10k was determined as a function of temperature and humidity. The insulin-PVP 10k system has a T_g value lower than that of the insulin-PVP K-30 system, such that the degradation rate can be determined at temperatures below and above T_g, allowing us to examine whether the temperature dependence of the rate changes around T_g. The temperature- and T_g-dependence of the degradation rate was analyzed to obtain the relative contributions of molecular mobility and the activational barrier.

EXPERIMENTAL

Lyophilization of Insulin

Lyophilization was carried out in a similar manner as reported previously.[1] Human zinc insulin (Humulin® RU-100, Eli Lilly & Co., Indianapolis, IN) was converted into the zinc-free neutral form by dialysis. PVP 10k (average molecular weight of 10k, Sigma Chemical Co., St. Louis, MO) was added to the solution to make a 5 mg/mL of PVP 10k solution and pH was adjusted to 4.0. The ratio of insulin to PVP 10k was 1:1.5 w/w. Four hundred microliters of the solution were frozen in a polypropylene sample tube (10 mm diameter), and then dried at a vacuum level below 5 Pa for 23.5 h in a lyophilizer (Freezevac C-1, Tozai Tsusho Co., Tokyo). The shelf temperature was between −35 and −30°C for the first 1 h, 20°C for the subsequent 19 h, and 30°C for the last 3.5 h.

Lyophilized samples were stored at 15°C for 24 h in a desiccator with a saturated solution of LiCl H_2O (12%RH), potassium acetate (23%RH), K_2CO_3 $2H_2O$ (43%RH), or NaBr $2H_2O$ (60%RH) to obtain samples with various T_g values.

Determination of T_g by Differential Scanning Calorimetry (DSC)

Modulated temperature DSC experiments were performed using a commercial system (2920; TA Instruments, DE) attached to a refrigerated cooling accessory. The conditions were as follows: modulation period of 100 s, a modulation amplitude of ±0.5°C, and an underlying heating rate of 1°C/min. Samples were put in a hermetic pan. Temperature calibration was performed using indium. The samples, pre-equilibrated at 12%RH, 23%RH, 43%RH, and 60%RH, exhibited a T_g value of 116°C, 88°C, 65°C, and 46°C, respectively. A representative DSC scan is shown in Figure 1. Change in heat flow corresponding to

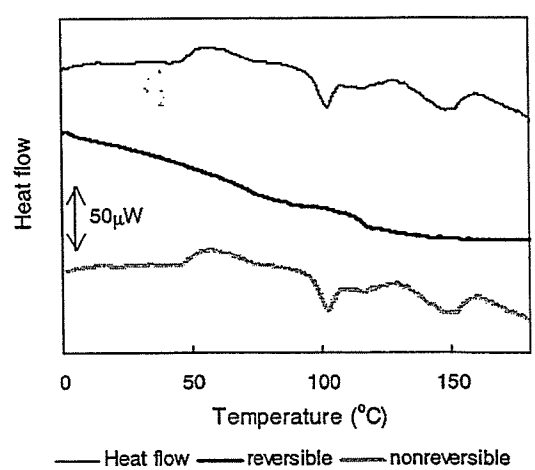

Figure 1. Modulated DSC scan for insulin lyophilized with PVP 10k (12%RH).

DOI 10.1002/jps

the T_g of PVP 10k alone was not observed, indicating no significant phase separation.

Measurement of Insulin Degradation by HPLC and High-Performance Size-Exclusion Chromatography (HP-SEC)

Lyophilized samples with various T_g values in tubes with a tight screw-cap were stored at a constant temperature (20–90°C), removed at various times, and stored in liquid nitrogen until assayed. Samples were dissolved in 1.5 mL of 0.01 M $(NH_4)_2SO_4$ (pH 2.2, adjusted with concentrated H_2SO_4) and each 20 μL aliquot of the solution (insulin concentration was 0.9 mg/mL) was subjected to reverse phase HPLC (RP-HPLC) and high-performance size-exclusion chromatography (HP-SEC), respectively.

The concentration of intact insulin was quantified using a modular RP-HPLC, as reported previously.[1] The column used was Inertsil WP-300 (C8, 4.6 mm × 250 mm, GL Science Inc., Tokyo) maintained at 35°C. Elutions were performed using a mixture of 0.01 M $(NH_4)_2SO_4$ (pH 2.2) and acetonitrile solution of 0.07% (v/v) trifluoroacetic acid (72.5:27.5) for 1 min. The ratio of the acetonitrile solution increased linearly from 27.5% to 30% in 15 min, 30% to 35% in 22 min. The detection wavelength was 214 nm.

The amount of insulin monomers was determined by a HP-SEC, as reported previously.[1] The column used was Protein-Pak 125 (7.8 mm × 300 mm, Waters, Milford, MA) maintained at 25°C. A 2.5 M acetic acid solution containing 4 mM L-arginine and 4% (v/v) acetonitrile was eluted at a rate of 1 mL/min. The chaotropic power of the mobile phase was assumed to be sufficient to disrupt all non-covalent interactions, so that covalent transamidation or other covalent bonding of insulin monomers to form dimer can be detected by the SEC.

RESULTS AND DISCUSSION

Figure 2 shows the time courses of insulin degradation in the insulin-PVP 10k system at 60%RH, determined by HPLC. Similar time courses were obtained at 12%RH, 23%RH, and 43%RH. Degradation in the initial stage was describable with first-order kinetics under all the temperature and humidity conditions studied, although the empirical Kohlrausch–Williams–Watts (KWW) equation (Eq. 5) could better fit the data exhibiting more than 10% degradation ($\beta_{KWW} = 0.5$). t_{90} was calculated from the apparent first-order constant in the initial stage according to Eq. 4. The time course for the amount of insulin monomers in the initial stage, determined by HP-SEC, was also describable with first-order kinetics under all the temperature and humidity conditions studied (data not shown).

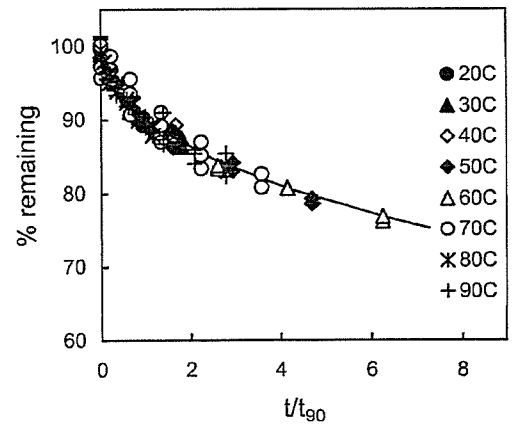

Figure 2. Time courses of insulin degradation at 60%RH and various temperatures measured by HPLC. Solid line represents the regression line obtained according to the KWW equation with a β_{KWW} value of 0.5.

$$\phi(t) = \exp\left[-\left(\frac{t}{\tau_{KWW}}\right)^{\beta_{KWW}}\right] \quad (5)$$

Figure 3 compares the t_{90} at 12%RH and 60%RH determined by HPLC with that determined by

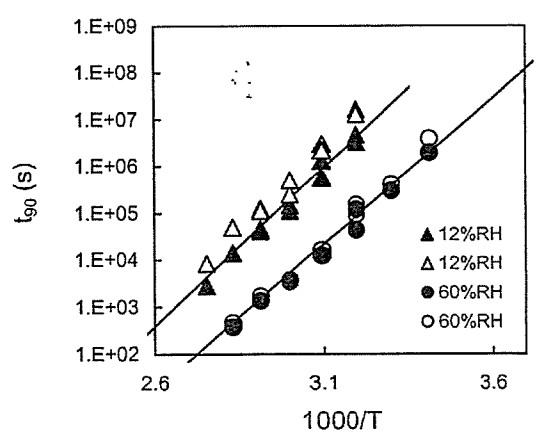

Figure 3. Comparison of t_{90} determined by HPLC (closed symbol) and that determined by HP-SEC (open symbol).

HP-SEC. The HPLC-derived t_{90} was significantly smaller than the SEC-derived t_{90} at 12%RH, whereas the difference was not significant at 60%RH. The t_{90} obtained at 23%RH and 43%RH (data not shown) indicated that the difference between HPLC-derived t_{90} and the SEC-derived t_{90} became less conspicuous as humidity increased. It has been observed that the major degradation pathways of insulin in acidic solution[4] and in lyophilized solids derived from acidic solutions[5] are A21-desamido insulin formation and dimerization via the cyclic anhydride intermediate. The same degradation pathways were observed in the insulin-PVP 10k system studied. A21-desamido insulin was identified based on the HPLC retention time coincident with that of the A21-desamido insulin prepared by the method reported.[6] Insulin dimer was detected by SEC. Formation of A21-desamido insulin, which reduces the HPLC insulin peak but not the SEC insulin peak, as well as insulin dimer formation can explain the SEC-derived t_{90} longer than the HPLC-derived t_{90}. The increase in the difference between the HPLC-derived t_{90} and the SEC-derived t_{90} with decreasing humidity is attributable to the decrease in molecular mobility that results in suppression of dimer formation.[5]

Figure 4 shows the temperature- and T_g-dependence of t_{90} obtained in the temperature range 20°C–90°C and the humidity range 12%RH–60%RH. The relative contributions to insulin degradation of molecular mobility and the chemical activational barrier were calculated by curve-fitting of the temperature- and T_g-dependence of the observed t_{90} to Eqs. 1 and 4. Solid lines in the figure represent the regression curves obtained. The value of k'/k was estimated to be unity (i.e., the value in parentheses in Eq. 1 was equal to unity), indicating that the significance of molecular mobility as a determinant for the reaction rate was small. As shown in Figure 4A, the t_{90} versus $1/T$ plots were not coincident for different humidity conditions, regardless of the negligible effect of molecular mobility. This finding suggests that ΔH varies with humidity. Curve-fitting provided ΔH estimates of 30.9, 30.5, 29.4, and 28.5 kcal/mol for 12%RH, 23%RH, 43%RH, and 60%RH, respectively, as well as A estimate of 10^{14}/s. Our previous paper[1] reported that ΔH for insulin degradation in insulin-PVP K-30 systems was estimated approximately 20 kcal/mol at 12%RH and 43%RH. However, recalculation after the removal of low-temperature data with large variations yielded ΔH estimates of approxi-

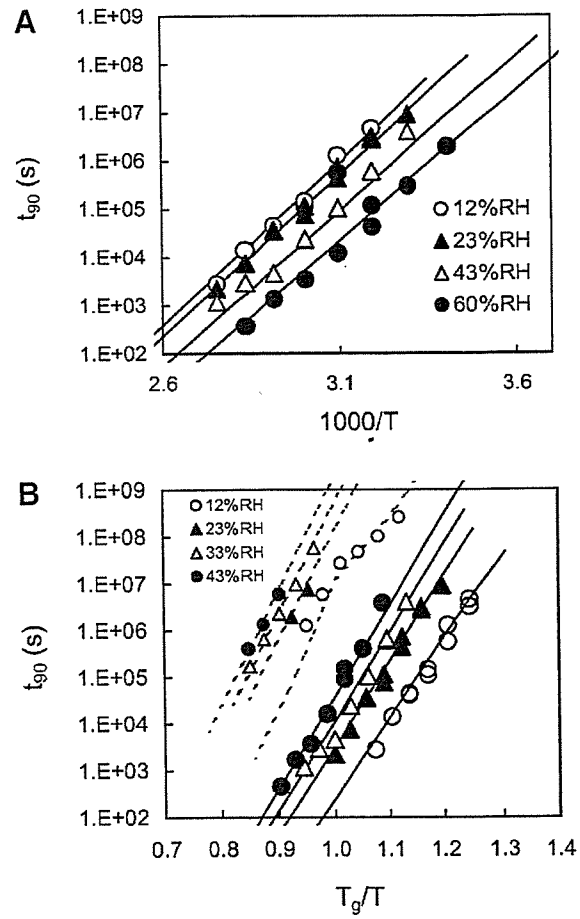

Figure 4. t_{90} of insulin degradation determined by HPLC plotted against $1/T$ (A) and T_g/T (B). Solid lines represent the regression lines obtained according to the Eq. 1. B: Further shows the t_{90} of degradation of insulin lyophilized with trehalose (small symbols and dotted lines), reported previously.[1]

mately 30 kcal/mol, which almost consisted with the ΔH estimated for insulin degradation in the insulin-PVP 10k system. This suggests that insulin degradation in the insulin-PVP K-30 system is due to A21-desamido formation and dimerization via the cyclic anhydride intermediate, similarly as in the insulin-PVP 10k system, rather than PVP-insulin adduct formation as speculated from the biased ΔH estimates in the previous paper.

The t_{90} versus T_g/T plots shown in Figure 4B exhibited no change in slope around T_g. Furthermore, the plots for different humidity conditions did not converge around T_g in a manner as expected when molecular mobility is a determinant for degradation rate (as shown in the previous simulation study[1]). These findings indi-

DOI 10.1002/jps

cate that molecular mobility is not a significant determinant for the degradation rate of insulin in the insulin-PVP 10k, as similarly observed in the insulin-PVP K-30 system. Thus, the speculation given rise to in the previous study,[1] that degradation rate is mainly governed by the chemical activational barrier rather than molecular mobility, was confirmed.

Figure 4B compares the temperature- and T_g-dependence of t_{90} for the insulin-PVP 10k system with that of the insulin-trehalose system reported previously.[1] The insulin-trehalose system exhibited a k'/k value (at T_g) larger than 0.9 at humidity levels above 23%RH and a k'/k value (at T_g) of 0.05 at 12%RH, indicating that molecular mobility is a major factor that determines the degradation rate at low humidity. In contrast, molecular mobility was found not to be a determinant for degradation rate in both the insulin-PVP 10k and insulin-PVP K-30 systems even at low humidity. The previous study[1] estimated ΔH of approximately 30 kcal/mol for insulin degradation in the insulin-trehalose systems at 23%RH, 33%RH, and 43%RH, which was close to the ΔH values estimated for degradation in the insulin-PVP 10k and K-30 systems. This finding suggests that the mechanisms for insulin degradation in the insulin-trehalose system is similar to that in the insulin-PVP 10k and K-30 systems (i.e., A21-desamido formation and dimerization via the cyclic anhydride intermediate). Further studies are required to explain why molecular mobility at 12%RH was lowered so as to become the rate-limiting step of the degradation pathway in the insulin-trehalose system, but not in the insulin-PVP 10k and K-30 systems. Interaction between proteins and sugars, which has been demonstrated by many studies, may be a possible explanation.

CONCLUSION

The temperature- and T_g-dependence of the degradation rate of insulin lyophilized with PVP 10k was analyzed by Eqs. 1 and 4 to obtain the relative contributions of molecular mobility and the chemical activational barrier. The results obtained at temperatures below and above T_g confirmed the speculation given rise to in our previous study that insulin degradation in the presence of PVP is mainly governed by the chemical activational barrier rather than molecular mobility.

REFERENCES

1. Yoshioka S, Aso Y. 2005. A quantitative assessment of the significance of molecular mobility as a determinant for the stability of lyophilized insulin formulations. Pharm Res 22:1358–1364.
2. Karel M, Saguy I. 1991. Effects of water on diffusion in food systems. Adv Exp Med Biol 302: 157–173.
3. Guo Y, Byrn SR, Zografi G. 2000. Physical characteristics and chemical degradation of amorphous quinapril hydrochloride. J Pharm Sci 89:128–143.
4. Darrington RT, Anderson BD. 1995. Effect of insulin concentration and self-association on the partitioning of A-21 cyclic anhydride intermediate to desamido insulin and covalent dimer. Pharm Res 12:1077–1084.
5. Strickley RG, Anderson BD. 1997. Solid-state stability of human insulin II. Effect of water on reactive intermediate partitioning in lyophiles from pH 2-5 solutions: Stabilization against covalent dimer formation. J Pharm Sci 86:645–653.
6. Darrington RT, Anderson BD. 1994. The The role of intramolecular nucleophilic catalysis and effects of self-association on the deamidation of human insulin at low pH. Pharm Res 11:784–793.

Molecular Mobility of Nifedipine–PVP and Phenobarbital–PVP Solid Dispersions as Measured by ^{13}C-NMR Spin-Lattice Relaxation Time

YUKIO ASO, SUMIE YOSHIOKA

Division of Drugs, National Institute of Health Sciences, 1-18-1, Kamiyoga, Setagaya, Tokyo 158-8501, Japan

Received 1 January 2005; revised 15 April 2005; accepted 25 August 2005

Published online 21 December 2005 in Wiley InterScience (www.interscience.wiley.com). DOI 10.1002/jps.20545

ABSTRACT: Amorphous nifedipine–PVP and phenobarbital–PVP solid dispersions with various drug contents were prepared by melting and subsequent rapid cooling of mixtures of PVP and nifedipine, or phenobarbital. Chemical shifts and spin-lattice relaxation times (T_1) of PVP, nifedipine, and phenobarbital carbons were determined by ^{13}C-CP/MAS NMR to elucidate drug–PVP interactions and the localized molecular mobility of drug and PVP in the solid dispersions. The chemical shift of the PVP carbonyl carbon increased as the drug content increased, appearing to reach a plateau at a molar ratio of drug to PVP monomer unit of approximately 1:1, suggesting hydrogen bond interactions between the PVP carbonyl group and the drugs. T_1 of the PVP carbonyl carbon in the solid dispersions increased as the drug content increased, indicating that the mobility of the PVP carbonyl carbon was decreased by hydrogen bond interactions. T_1 of the drug carbons increased as the PVP content increased, and this increase in T_1 became less obvious when the molar ratio of PVP monomer unit to drug exceeded approximately 1:1. These results suggest that the localized motion of the PVP pyrrolidone ring and the drug molecules is reduced by hydrogen bond interactions. Decreases in localized mobility appear to be one of the factors that stabilize the amorphous state of drugs.
 J Pharm Sci 95:318–325, 2006
Keywords: spin-lattice relaxation time; amorphous; solid dispersion; stability; molecular mobility

INTRODUCTION

To improve their dissolution rate and solubility, poorly soluble drugs are used in the amorphous form. However, drugs in the amorphous form are generally less stable than crystalline drugs because of their higher energy state and higher molecular mobility. It is well known that poly (vinylpyrrolidone) (PVP) can reduce the crystallization rate of many amorphous drugs.[1–10] This stabilization by PVP is partly attributed to its ability to decrease molecular mobility, as indicated by increases in the glass transition temperature (T_g).[9] Observations of increases in the enthalpy relaxation time of amorphous drugs in the presence of small amounts of PVP also suggest decreases in molecular mobility.[2,7,10] We have reported that the overall crystallization rates of amorphous phenobarbital or nifedipine were reduced by 2–3 orders of magnitude by addition of a small amount of PVP, and that amorphous phenobarbital was stabilized more effectively by PVP than was amorphous nifedipine.[10] The enthalpy relaxation time of amorphous nifedipine increased from 1.2 to 18 days in the presence of 10% PVP, whereas that of amorphous phenobarbital increased from 1.0 to 3.7 days in the presence of 5% PVP. The enthalpy relaxation times of the solid dispersions, however, do not seem to be long

Correspondence to: Yukio Aso (Telephone: +81-3-3700-8547; Fax: +81-3-3707-6950; E-mail: aso@nihs.go.jp)

Journal of Pharmaceutical Sciences, Vol. 95, 318–325 (2006)

enough to explain fully the large increases in stability of the amorphous drugs.

Hydrogen bond interactions between PVP and drugs have been detected by FT–IR,[2,11] FT–Raman[12–15], and water vapor sorption[16,17] measurements, and may be one of the factors involved in stabilization of amorphous drugs by PVP.[2,4–8,11] It is of great interest to elucidate the effects of hydrogen bond interactions on the mobility of drug molecules in amorphous solid dispersions. Shamblin and Zografi studied the effects of hydrogen bond interactions on the molecular mobility of amorphous sucrose by measuring the enthalpy relaxation of amorphous sucrose in the presence of dextran, PVP, poly(vinylpyrrolidone-co-vinyl acetate), or trehalose. Although the T_g values of the sucrose-additive mixtures studied were similar to that of sucrose, the rate of enthalpy relaxation of sucrose was smaller after addition of additives with higher T_g values. The decreased molecular mobility of sucrose was attributed to interactions that led to coupling of the molecular motions of sucrose and of the additives.[18] Measuring the mobilities of drug and additive molecules as a function of additive content may be useful to elucidate the effects of hydrogen bond interactions on molecular mobility. Enthalpy relaxation measurements, however, seem not to be applicable for this purpose, since the T_g of the drug-additive mixtures would change as the additive content increased and comparison of the enthalpy relaxation times of the mixtures would be difficult.

^{13}C-CP/MAS NMR measurements may be particularly useful for such investigations, because knowledge of ^{13}C-NMR spin-lattice relaxation times (T_1) can indicate the molecular mobility of each compound in multi-component systems.[19–22] Hydrogen bond interactions of PVP may also be detected from changes in the chemical shift of the PVP carbonyl carbons, in a similar manner to that of the poly(3-hydroxybutyrate) carbonyl carbon in the presence of polyvinyl alcohol.[23]

In this paper, T_1 and chemical shift values of PVP and drug carbons in nifedipine–PVP and phenobarbital–PVP solid dispersions with various PVP contents were determined by ^{13}C-CP/MAS NMR in order to elucidate the effects of hydrogen bond interactions on the molecular mobility of amorphous nifedipine and phenobarbital. The characteristics of the interaction between nifedipine and PVP were compared with those of the interaction between phenobarbital and PVP to explain the differences in the ability of PVP to stabilize the two drugs.

EXPERIMENTAL

Materials

Nifedipine (melting point 172°C) and PVP (PVP-40, Mw 40000) were purchased from Sigma (St. Louis, MO) and used as received. Phenobarbital was prepared from sodium phenobarbital (Wako Pure Chemical Ind., Osaka, Japan) according to a previously described method.[24] Shortly, phenobarbital was precipitated from aqueous sodium phenobarbital solution by neutralization. The precipitate obtained was then crystallized from acetone solution. The melting point of the crystalline phenobarbital was observed at 175°C by DSC, consistent with that reported previously.[24] The peak area of the crystalline phenobarbital in high performance liquid chromatogram was confirmed to be equivalent to that of sodium phenobarbital.

Preparation of Nifedipine–PVP and Phenobarbital–PVP Solid Dispersions

Nifedipine–PVP and phenobarbital–PVP solid dispersions were prepared by melting and subsequent rapid cooling of mixtures of each drug and PVP. Nifedipine or phenobarbital were dissolved in methanol with PVP at various weight ratios. The methanol was then evaporated off with a rotary evaporator under reduced pressure. The mixture thus obtained was ground in a mortar and then dried in a vacuum chamber at about 60°C for 1 day. The dried mixtures were heated at approximately 180°C for 10–20 min in a Teflon vessel and then were cooled by immersion in liquid nitrogen. The amorphous nature of each sample was confirmed by glass transition temperature (T_g) measurements and observation under polarized light. T_g measurements were carried out using a 2920 differential scanning calorimeter (DSC) and the refrigerator cooling system (TA instrument, New Castle, DE). The modulated temperature program used was ±0.5°C modulation amplitude within 100 s and an underlying heating rate of 1°C/min. Hermetic aluminum sample pans were used for measurement. Temperature and cell constant calibration of the instrument was carried out using indium. DSC cell was purged by dry nitrogen (30 mL/min). Table 1 shows the T_g of nifedipine– and phenobarbital–PVP solid dispersions. Single glass transition temperature was observed for all the samples studied, indicating that the dispersions were amorphous.

Table 1. T_g of Nifedipine–PVP and Phenobarbital–PVP Solid Dispersions

	T_g (°C)[a]
Nifedipine	41.9 ± 0.4
Nifedipine–PVP 90:10	43.5 ± 1.0
Nifedipine–PVP 80:20	51.9 ± 0.1
Nifedipine–PVP 70:30	69.5 ± 0.8
Nifedipine–PVP 50:50	96.9 ± 0.4
Nifedipine–PVP 30:70	124.9 ± 0.7
Phenobarbital	40.8 ± 0.2
Phenobarbital–PVP 90:10	46.5 ± 0.1
Phenobarbital–PVP 80:20	57.7 ± 0.2
Phenobarbital–PVP 65:35	89.6 ± 0.5
Phenobarbital–PVP 50:50	115.3 ± 0.9
Phenobarbital–PVP 70:30	135.5 ± 0.6
PVP	168.2 ± 0.6

[a]Average and standard deviation of the mid-point T_g ($n = 3$).

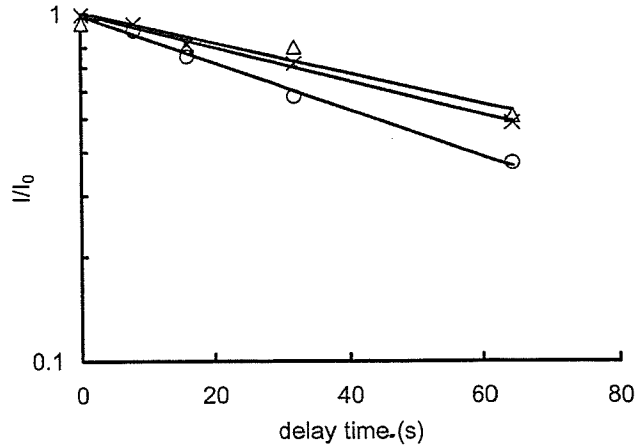

Figure 1. Typical signal decay of the PVP carbonyl carbon. ○, pure PVP; △, nifedipine–PVP (8:2); ×, phenobarbital–PVP (8:2).

^{13}C High-Resolution Solid State NMR

NMR measurements were carried out using freshly prepared samples in order to minimize the possible effect of enthalpy relaxation on the T_1. The amorphous samples obtained were very gently pulverized by using a spatula and, avoiding mechanical stress, put into NMR rotors. The NMR sample preparation was carried out in a grove bag filled with dry nitrogen in order to avoid water sorption by samples. The water content of the samples was determined to be less than 0.1 w/w% by the Karl–Fisher method. NMR measurements were carried out at 27°C with a Varian Unity plus spectrometer (Varian, Inc., Palo Alto, CA) at a proton resonance frequency of 400 MHz. The chemical shift calibration of the instrument was conducted with hexamethylbenzene (methyl group at 17.3 ppm) as an external standard. The pulse sequence for T_1 measurement was that reported by Torchia.[25] The spinning rate was 6.5 kHz, the contact time was 1 ms, delay time was 0.1, 8, 16, 32, 64 s, and recycling delay was 5 s. Scans (400–500) were accumulated for each spectrum. Signals were assigned according to chemical shift data reported for PVP, nicardipine, nimodipine, nifedipine, and phenobarbital glucoside.[19,26–30] Nifedipine carbons observed at 103 ppm were assigned to be C-2 and C-6 carbons[26,27] or C-3 and C-5 carbons.[29] Figure 1 shows the typical signal decay of the PVP carbonyl carbon. When the PVP carbonyl group interacts with drugs, signal decay is expected to be describable by the sum of two or more exponential functions, since there are at least two types of PVP carbonyl carbons with different molecular mobilities. It was, however, difficult to separate the signal decay into two exponential functions, since differences in T_1 were small, as shown in Figure 1. Therefore, the signal decay of all carbons was described by a single exponential function and apparent T_1 values were reported in this paper. There was no significant change in DSC thermograms, suggesting no crystallization occurring in the solid dispersion samples after NMR measurements.

RESULTS AND DISCUSSION

Effect of Drug Content on Chemical Shift and T_1 of PVP Carbons

Figures 2 and 3 show typical ^{13}C-CP/MAS NMR spectra of nifedipine–PVP and phenobarbital–PVP solid dispersions. The chemical shift of the PVP carbonyl carbon, observed at approximately 175 ppm, increased in the presence of nifedipine or phenobarbital. For the phenobarbital–PVP solid dispersion, the chemical shift of C-2 carbon of PVP decreased from 19.5 ± 0.1 ppm to 19.0 ± 0.2 ppm. In contrast, the chemical shift of PVP carbons other than the carbonyl carbon did not change within experimental error for the nifedipine–PVP solid dispersions. Figure 4 shows the effects of drug content on the chemical shift of the PVP carbonyl carbon. The chemical shift

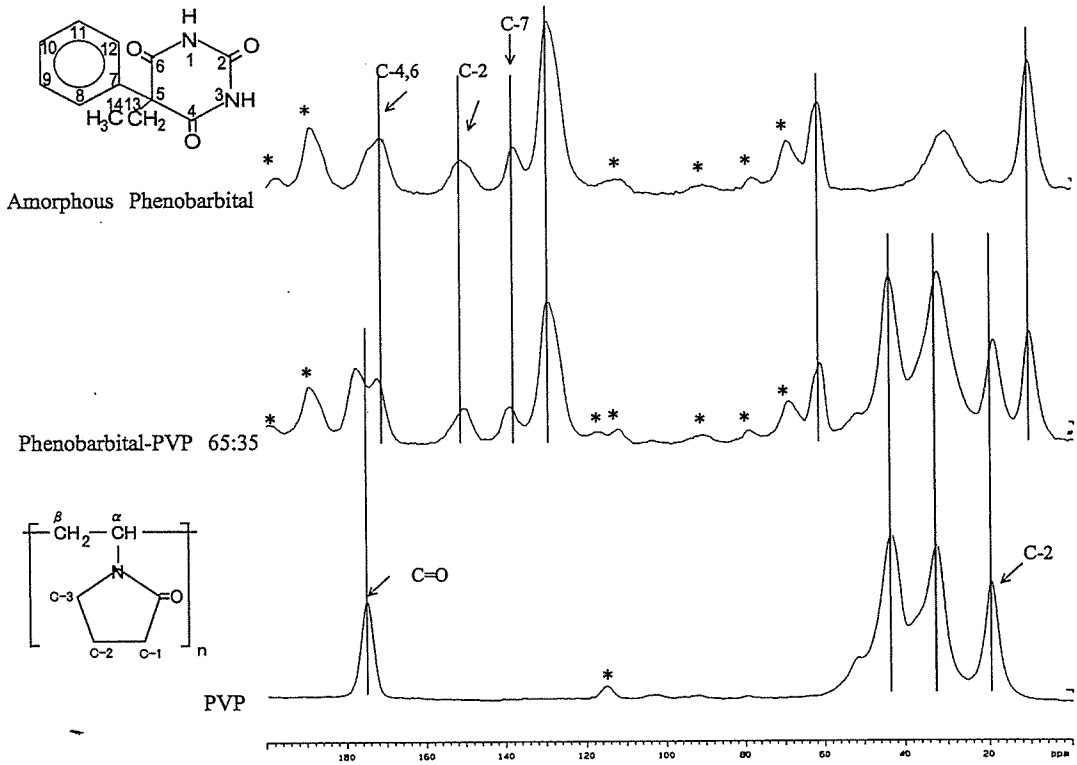

Figure 2. Typical ^{13}C CP/MAS spectra of amorphous phenobarbital–PVP. * represents spining side bands.

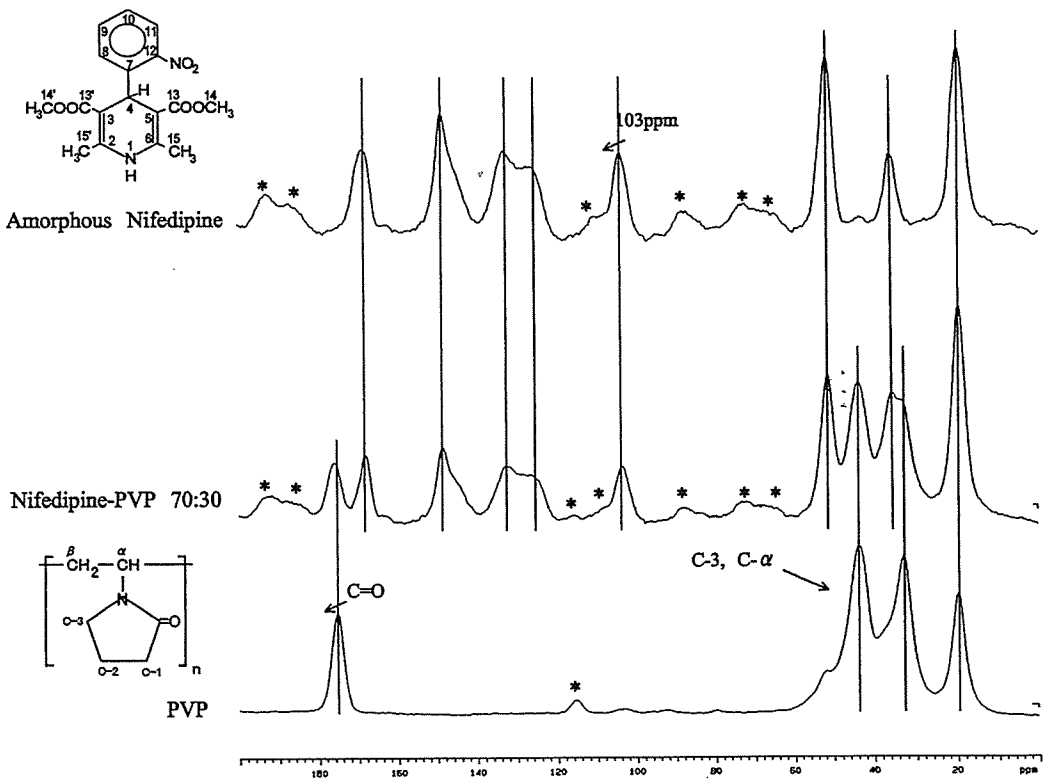

Figure 3. Typical ^{13}C CP/MAS spectra of amorphous nifedipine–PVP. * represents spining side bands.